

The Enigmatic Permanganate Ion: An Accurate Protocol for Modelling Absorption Spectra of Solvated Transition Metal Ions.

Jógvan Magnus Haugaard Olsen^{*,†} and Erik Donovan Hedegård^{*,‡}

*Department of Physics, Chemistry and Pharmacy, University of Southern Denmark, Campusvej
55, DK-5230 Odense M, Denmark, and Department of Chemistry, Lund University, Kemicentrum
Sölvegatan 39, Lund, Sweden*

E-mail: jmo@sdu.dk; erik.hedegard@teokem.lu.se

*To whom correspondence should be addressed

†University of Southern Denmark

‡Lund University

Abstract

The absorption spectrum of the MnO_4^- ion has been a test-bed for quantum chemical methods over the last decades. Its correct description requires highly correlated multiconfigurational methods, which due to their high computational demands, are incompatible with inclusion of finite-temperature effects and explicit solvent interactions. Therefore, implicit solvent models are employed instead. Here we show that implicit solvent models are not sufficiently accurate to model the solvent shift of MnO_4^- , and we analyze the origins of their failure. We obtain a correct solvent shift for MnO_4^- by employing an explicit, polarizable embedding (PE) model, where we describe MnO_4^- with a range-separated, multiconfigurational short-range density functional theory method (“CAS-srDFT”). The underlying structures are obtained from ab initio molecular dynamics. The explicit treatment of the solvent facilitates the interpretation of the bands in the low-energy region of the MnO_4^- absorption spectrum, whose assignment until now has been elusive.

Introduction

Inclusion of environment effects in computational chemistry is pivotal to achieve the best possible match between theoretical models and experimental measurements. In particular, absorption spectra can be sensitive to the presence of a molecular environment, and many chemical compounds have a characteristic shift of their excitation energies that depends on the specific environment. For solutes, the *solvent shift* may be defined as $\Delta E_{\text{shift}} = E_{\text{sol}} - E_{\text{vac}}$, where E_{sol} and E_{vac} are excitation energies obtained with or without solvent included, respectively. An accurate prediction of excitation energies and solvent shifts poses special demands on the theoretical model. First, the perturbation of the solute’s charge density induced by the environment must be accurately modeled. Further, it is necessary to include finite-temperature effects e.g. by averaging over several structures from a molecular dynamics (MD) trajectory. An additional complication arises when the solute is a transition metal complex, which can generally be expected to display multireference character. In such cases both dynamical and static correlation must be modeled accurately

with multiconfigurational methods, such as complete active space second-order perturbation theory (CASPT2).¹ Unfortunately, such methods are plagued by very high computational costs. A prime example is the MnO_4^- ion, whose absorption spectrum has been a test-bed for semi-empirical ligand field theory² and quantum chemical methods,³⁻¹⁴ alike for the last decades. Despite its apparent simplicity, the closed-shell (d^0) MnO_4^- ion, has been shown to have sizable non-dynamical correlation.¹⁵ Ab initio methods based on a single-reference wave function have resulted in different assignments^{4-6,8,13} of the experimental spectrum.¹⁶ The ubiquitous time-dependent density functional theory (TD-DFT) has also been applied, but is noted to significantly overestimate the absolute excitation energies,^{7,9,10} although recent development by Ziegler and co workers seems to offer some improvement.¹⁴ An obstacle for the application of multireference methods has been that the required active space has been estimated to be 24 electrons in 17 orbitals, which is rather large.¹⁷⁻¹⁹ A recent study of the MnO_4^- electronic absorption spectrum managed to reach the required active space with a restricted active space method (RASPT2).²⁰ Although good agreement with experimental was obtained, the study did not consider finite-temperature effects.

Despite the long history of MnO_4^- , it continues to cause controversy. Transitions in the low-energy region are still not assigned,^{16,21} and with the recent measurement of accurate gas-phase data,²¹ experimental estimates of the ΔE_{shift} for the first, second and third electronic bands are available; all are small blue-shifts (i.e. $\Delta E_{\text{shift}} > 0$). For the first band, previous theoretical studies employing continuum solvation models predicted either a negligible solvent shift of -0.01 eV²⁰ or a somewhat more pronounced red-shift of -0.13 eV,^{10,22} in clear contrast to experiment. It is presently not known whether the discrepancies are caused by inadequate electronic structure methods, solvent models, or both.

Here we advocate the use of a method that combines Kohn-Sham (KS) density functional theory (DFT) with a multireference wave function. A number of such schemes are currently in development²³⁻⁴¹ and here we employ a range-separation method denoted complete active space short-range DFT (CAS-srDFT).^{27,28,31-33,35} The CAS-srDFT method is computationally cheaper than perturbation-based multireference methods and has been shown to be of comparable accu-

racy.^{34–36} Further, its simultaneous treatment of dynamical and static correlation enables the use of significantly smaller active spaces without much loss in accuracy. We exploit this here to go beyond what have been done so far, and also consider finite-temperature effects as well as the direct, electronic solvent effects on the absorption spectrum. Thus, we calculate CAS-srDFT excitation energies and oscillator strengths using a series of structures taken from ab initio MD and combined quantum mechanics / molecular mechanics (QM/MM) MD simulations. From these underlying structures we also show that continuum solvation models describe the electrostatic perturbation by the solvent incorrectly. We will instead employ the polarizable embedding (PE) model^{42,43} which uses an advanced, classical potential to model the electronic solvent effects. With the combined use of MD and PE-CAS-srDFT,⁴⁴ we are able to reproduce the experimentally-obtained blue shift reasonably well. Furthermore, can assign the low-energy parts of the MnO_4^- absorption spectrum.

Results

Before investigating the MnO_4^- ion in an explicit solvent, we investigate the performance of the CAS-srDFT method on the MnO_4^- ion in vacuum and in implicit, aqueous solvent. In this study, we investigate the four lowest intense transitions in T_d symmetry (i.e. transitions to the T_2 states).

We employ symmetric, geometry-optimized structures, i.e., we neglect finite-temperature effects, and include solvent effects via the polarizable continuum model (PCM). We have performed the calculations based on two geometries: a vacuum geometry (BLYP/6-31G) and a solvent (PCM) geometry (PCM-BLYP/6-31G). For each structure, the lowest excitation energies, as well as the associated oscillator strengths, were obtained based on time-dependent CAS(14,12)-srPBE calculations, both with and without the PCM embedding. By this procedure, we separate the solvent effects on the spectrum into the direct contribution stemming from the electrostatic interactions between the solute electrons and the solvent, and the indirect contribution which is the solvent-induced change in geometry. The results are shown in 1. The CAS-srPBE calculation on the vacuum geometry are the values (shown in the second column of 1) that can be compared to the

accurate results based on RASPT2.²⁰ Both RAS(24,17)PT2 and CAS(14,12)-srPBE are within

Table 1: Excitation energies (in eV) and oscillator strengths (in parentheses) of the lowest intense transitions of the MnO_4^- ion in vacuum (E_{vac}) and aqueous solution (E_{sol}) calculated using geometry-optimized structures

Method	CAS(14,12)-srPBE ^a		PCM ^b -CAS(14,12)-srPBE ^a		RAS(24,17)PT2 ^c	expt ^d
Geom.	vacuum	PCM	vacuum	PCM	vacuum	-
State	$E_{\text{vac}}(f)$	$E_{\text{vac}}(f)$	$E_{\text{sol}}(f)$	$E_{\text{sol}}(f)$	$E_{\text{vac}}(f)$	$E_{\text{exp}}(I)$
1^1T_2	2.21 (0.095)	2.25 (0.092)	2.16 (0.127)	2.20 (0.123)	2.33 (0.004)	2.2 (s)
2^1T_2	3.61 (0.010)	3.64 (0.010)	3.61 (0.018)	3.64 (0.018)	3.53 (0.002)	3.6 (m)
3^1T_2	4.01 (0.084)	4.05 (0.082)	-	-	4.20 (0.006)	4.1 (s)
4^1T_2	5.13 (0.171)	5.19 (0.162)	-	-	5.71 (0.002)	≈ 5.4 (m)

^a Calculated in a modified version of DALTON with cc-pVDZ basis set and a the srPBE(HSE;RI) exchange-correlation functional,⁴⁵ defined as done in Ref. 27. ^b Cavity was built using 1.9 and 1.52 Å for Mn and O atomic radii, respectively. ^c Values from ref. 20. ^d Values from ref. 16. Relative intensities indicated in parentheses (s = strong, m = medium).

0.01–0.1 eV of the experimental value for the first three excitations. The largest difference is seen for the fourth state, where CAS(14,12)-srPBE underestimates the excitation with about 0.3 eV, whereas RAS(24,17)PT2 overestimates with the same margin. The oscillator strengths for this state are also rather different. The latter is not unprecedented, as we recently showed that CASPT2 and CAS-srDFT can obtain oscillator strengths that differ significantly,³⁴ although they usually predict the same trends. Some of the differences have been attributed to the fact that oscillator strengths in CASPT2 (and RASPT2) methods are effectively obtained at the CASSCF level.³⁴ We note that Su et al.²⁰ actually report two states with low oscillator strength below 4^1T_2 , and the state that we have here assigned 4^1T_2 is actually 6^1T_2 in Ref. 20. For these higher lying excitations (close to the ionization limit) the inclusion of Rydberg basis sets can be of importance, although it had only little effect in Ref. 20. However, CAS-srDFT has previously been noted to be more sensitive than e.g. CASPT2 to Rydberg-valence mixing.^{35,36}

The results from the PCM-CAS-srPBE calculation on the PCM geometry, are in the fifth column of 1, whereas the values in the third and fourth columns can be considered as intermediates between vacuum and solvent. The most consistent estimations of the solvent shifts (ΔE_{shift}) are obtained as the difference between PCM-CAS-srPBE values using the PCM geometry and the

CAS-srPBE values using the vacuum geometry, i.e., from the second and fifth column of 1. However, previous theoretical studies of MnO_4^- have occasionally neglected the indirect geometry effect of the solvent.^{10,22} The shift of -0.14 eV reported in Ref. 10 is based on an E_{vac} that was obtained from a structure optimized in vacuum (BPW91/TZ2P), whereas E_{sol} was from the work by Seth et al.²² where COSMO-SAOP/TZ2P was used on a structure optimized in vacuum (BP86/TZ2P). Meanwhile, the small shift (0.01 eV) reported by Su et al.²⁰ was obtained with SAOP/TZ2P and COSMO. If both structure and excitation energy are obtained consistently, then our estimate of the solvent shift (ΔE_{shift}) is only -0.01 eV, which is in good agreement with the shift obtained by Su et al.²⁰ but differs somewhat from the red-shift of -0.14 eV reported in Ref. 10. Seeing that we here also obtain a small red-shift of -0.05 eV when using only structures optimized in vacuum (columns 3 and 1 in 1), the discrepancy can, at least partly, be explained by the neglect of indirect solvent effects. All the same, even with a consistent model, continuum models alone do not seem to be able to reproduce the experimental blue-shift of 0.10 ± 0.01 eV.²¹

We now move to consider an explicit solvent environment. We computed the absorption spectra based on the twelve lowest states and in 2 we report E_{vac} and E_{sol} for these twelve states as averages based on 80–100 structures, taken from an MD trajectory. Convolution of these states into a Gaussian spectrum leads to the spectrum shown in 1. The two peaks corresponds to the two lowest intense bands in of ${}^1\text{T}_2$ parentage (i.e. 1^1T_2 and 2^1T_2 for the symmetric structures in 1). However, the perturbation induced by the solvent molecules as well as the finite-temperature effects remove the degeneracy of the T_1 and T_2 states. Thus, the T_1 and T_2 states are split into six states in total. Further, the transition to the T_1 state is dipole forbidden in T_d symmetry, but gains intensity when the symmetry is removed by finite-temperature effects and solvent interactions. The peak-maxima in 1 are used to calculate ΔE_{shift} , given in 3. We start by discussing these, and thereafter we will provide a more detailed analysis of the individual states in 2.

From the spectrum we obtain an excitation energy of 2.25 eV for the 1^1T_2 state in vacuum. This is 0.04 eV higher than than the energy obtained using the geometry-optimized structure (see 1) which can be attributed to finite-temperature effects in the ground-state. The PCM predicts a

Table 2: Excitation energies and oscillator strengths of the twelve lowest intense transitions of the MnO_4^- ion in vacuum or in aqueous solution^a

Geom. Environment		QM MD ^b vacuum		vacuum ^f		QM/MM MD ^c PCM ^{d,g}		PE ^{e,h}	
Multiplet	State	E_{vac} (eV)	f	E_{sol} (eV)	f	E_{sol} (eV)	f	E_{sol} (eV)	f
1T ₁	1	1.93	0.013	1.97	0.008	1.98	0.011	1.91	0.010
	2	2.03	0.005	2.07	0.005	2.07	0.008	2.04	0.003
	3	2.08	0.006	2.13	0.007	2.13	0.008	2.14	0.006
1T ₂	4	2.19	0.014	2.23	0.017	2.22	0.015	2.30	0.016
	5	2.29	0.019	2.34	0.018	2.32	0.019	2.45	0.014
	6	2.41	0.016	2.46	0.016	2.44	0.019	2.55	0.012
2T ₁ /2T ₂	7	3.36	0.002	-	-	3.42	0.003	3.33	0.003
	8	3.39	0.002	-	-	3.45	0.002	3.40	0.003
	9	3.42	0.002	-	-	3.48	0.002	3.45	0.003
	10	3.46	0.002	-	-	3.52	0.002	3.50	0.002
	11	3.49	0.002	-	-	3.56	0.002	3.55	0.003
	12	3.54	0.004	-	-	3.61	0.006	3.61	0.004

^a Calculated in a modified version of DALTON with CAS(14,12)-srPBE/cc-pVDZ with the srPBE(HSE;RI) exchange-correlation functional,⁴⁵ defined as done in Ref. 27. ^b Averages based on 100 structures taken from 1.0 ns BLYP/6-31G MD trajectory, calculated with TeraChem. ^c Averages based on 100 structures taken from ten 0.1 ns BLYP/6-31G//TIP3P MD trajectories, calculated with TeraChem. ^d Cavity was built using 1.9 and 1.52 Å for Mn and O atomic radii, respectively. ^e Embedding potential based on B3LYP/cc-pVDZ calculations ^f Based on 87 structures ^g Based on 87 structures ^h Based on 99 structures

Table 3: Absorption maxima and solvent shifts of the two lowest bands of MnO_4^- ion, calculated from the spectrum in 1. All results are based on CAS(14,12)-srPBE.

Band	PCM	PE	Exp. ²¹
1st	187 (0.02)	1226 (0.15)	800±70 (0.10±0.01)
2nd	625 (0.08)	366 (0.05)	740 (0.09) ^a

^a From data obtained in the crystalline phase.^{16,21}

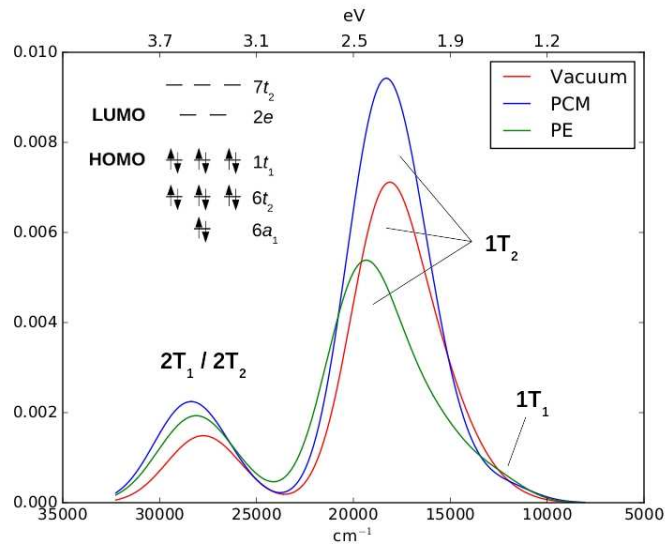


Figure 1: Simulated spectra of the MnO_4^- ion in vacuum and aqueous solution modeled by PCM or PE. The absorption maxima are: 18116 cm^{-1} (2.25 eV) and 27748 cm^{-1} (3.44 eV) in vacuum, 18303 cm^{-1} (2.27 eV) and 28373 cm^{-1} (3.52 eV) in PCM, 19342 cm^{-1} (2.40 eV) and 28114 cm^{-1} (3.49 eV) in PE. The insert shows the generally accepted frontier molecular orbital diagram, labeled according to the T_d point group.

very small blue-shift of 0.02 eV (see 3) which, albeit small compared to experimental shift, at least is the right direction, contrary to the previously reported red-shifts.^{10,21,22} The PE model predicts a larger blue-shift of 0.15 eV (see 3), which is slightly overestimated but closer to the experimental shift than the shift predicted by the PCM.

Next, we break down the spectrum in 1 into the individual states given in 2. We can compare these to the results obtained with a symmetric structure in 1. We should note that we for the symmetric structure in 1 obtain an excitation energy of 2.13 eV for the 1^1T_1 multiplet (not shown in 1), and with the excitation energy of 2.21 eV for the 1^1T_2 state (1), the splitting of the 1^1T_1 and 1^1T_2 states in vacuum is only 0.11 eV, similar to results with RASPT2.²⁰ With such a small energy-gap, the two states are expected to mix when the tetrahedral symmetry is lifted. This is indeed the case, but among the lowest six states, the 1^1T_1 and 1^1T_2 multiplets can still be discerned (cf. 2). The three states of 1^1T_1 parentage are still lower than the intense 1^1T_2 band, and can also be discerned in the spectrum in 1, as a weak transition at approximately 1.7-1.9 eV ($13700\text{--}15300\text{ cm}^{-1}$) prior to the large peak from 1^1T_2 . Low-intensity peaks have indeed previously been

observed in MnO_4^- spectra around 1.8 eV.^{16,21} Analysis have suggested that their origin were either in spin-forbidden $^3\text{T}_2$, orbital forbidden $^1\text{T}_1$ states, or both.⁴⁶⁻⁴⁸ From our calculations here, we cannot exclude the involvement of triplet states, but our results show that the $^1\text{T}_1$ states are likely to gain sufficient intensity to be responsible for the observed low-intensity band. This assignment can naturally not be extracted from previous vacuum studies^{10,20,22} with symmetric structures, where the intensity of the T_1 states are identically zero.

From inspection of 2 we also observe that the direct electrostatic effect of the solvent is predicted different by the PE model compared to the PCM. In both cases, the (indirect) solvent effect coming from the change in geometry of the solvated MnO_4^- ion, results in a blue-shift of the excitation energies. This can be seen in 2 by comparing the excitation energies based on QM MD geometries to QM/MM MD geometries (both with vacuum environment, columns 3 and 5). For the PCM the direct solvent effects (obtained from column 5 and 7 in 2) is a (small) red-shift of the excitation energies. Adding this to the indirect solvent shift thus give the very small blue-shift as discussed above. Meanwhile, the direct solvent effects modeled by the PE model (cf. column 5 and 9 in 2) is a blue-shift of the excitation energy, leading to a more pronounced total blue-shift.

We can also briefly comment on the higher lying states in 2 and 1. Our CAS-srPBE results from the symmetric structure in 1 showed that the dipole-allowed 2^1T_2 multiplet is just above the dipole-forbidden 2^1T_1 multiplet: The excitation energy of the former is 3.61 eV (see 1) whereas the 2^1T_1 multiplet has an excitation energy of 3.48 eV (not shown in 1). The RASPT2 results from Ref. 20 predict a similar situation where the excitation energies are 3.53 eV (2^1T_1) and 3.39 eV (2^1T_2), respectively. These two multiplets are mixed when including finite-temperature and solvent effects and can no longer be discerned (cf. 2). From the spectra in 1 we obtain an excitation energy of 3.44 eV in vacuum, and blue-shifts of 0.08 and 0.05 for the PCM and the PE model, respectively (see 3). There is no experimental value for this transition in aqueous solution but a value exists for a crystalline phase. Using this value as reference, both solvent models yield a qualitatively reasonable shift (cf. 3).

It should finally be noted that we do not reproduce the vibrational structure of the spectrum,

since our underlying structures only include vibrations from the electronic ground state, while the significant vibrational structure in the MnO_4^- spectrum is a result of vibrational coupling in the excited states. Although the absolute excitation energies are significantly overestimated by the TD-DFT results presented in Ref. 10 (as also noted by the authors), TD-DFT convincingly reproduces the vibrational structure through an effective Hamiltonian approach. Employing a similar model for CAS-srDFT would be an interesting extension of our current approach and is left for further studies. The good agreement with experiment obtained here is encouraging for further investigating the PE-CAS-srDFT method for other transition metals, both in solution and in protein systems.

Acknowledgement

J.M.H.O. acknowledges financial support from the Danish Council for Independent Research (DFR) through the Sapere Aude research career program (Grant no. DFR-1323-00744 and DFR-1325-00091). E.D.H thanks the Carlsberg and Villum Kann Rasmussen foundations for funding.

References

- (1) Andersson, K.; Malmqvist, P.; Roos, B. O. *The Journal of Chemical Physics* **1992**, *96*, 1218–1226.
- (2) Wolfsberg, M.; Helmholz, L. *The Journal of Chemical Physics* **1952**, *20*, 837–843.
- (3) Johnson, K.; Smith, F. J. *Chemical Physics Letters* **1971**, *10*, 219–223.
- (4) Johansen, H.; Rettrup, S. *Chemical Physics* **1983**, *74*, 77–81.
- (5) Nakai, H.; Ohmori, Y.; Nakatsuji, H. *J. Chem. Phys.* **1991**, *95*, 8287–8291.
- (6) Nooijen, M. *J. Chem. Phys.* **1999**, *111*, 10815–10826.
- (7) van Gisbergen, S. J. A.; Groeneveld, J. A.; Rosa, A.; Snijders, J. G.; Baerends, E. J. *The Journal of Physical Chemistry A* **1999**, *103*, 6835–6844.

- (8) Nooijen, M.; Lotrich, V. *The Journal of Chemical Physics* **2000**, *113*, 494–507.
- (9) Boulet, P.; Chermette, H.; Daul, C.; Gilardoni, F.; Rogemond, F.; Weber, J.; Zuber, G. *The Journal of Physical Chemistry A* **2001**, *105*, 885–894.
- (10) Neugebauer, J.; Baerends, E. J.; Nooijen, M. *The Journal of Physical Chemistry A* **2005**, *109*, 1168–1179.
- (11) Jose, L.; Seth, M.; Ziegler, T. *The Journal of Physical Chemistry A* **2012**, *116*, 1864–1876.
- (12) Ziegler, T. *Struct. Bond* **2012**, *143*, 1–38.
- (13) Almeida, N. M.; McKinlay, R. G.; Paterson, M. J. *Chemical Physics* **2015**, *446*, 86–91.
- (14) Seidu, I.; Krykunov, M.; Ziegler, T. *Journal of Chemical Theory and Computation* **2015**, *11*, 4041–4053, PMID: 26575900.
- (15) Buijse, M. A.; Baerends, E. J. *The Journal of Chemical Physics* **1990**, *93*, 4129–4141.
- (16) Holt, S. L.; Ballhausen, C. *Theoretica chimica acta* **1967**, *7*, 313–320.
- (17) Veryazov, V.; Malmqvist, P. J.; Roos, B. O. *International Journal of Quantum Chemistry* **2011**, *111*, 3329–3338.
- (18) Hedegård, E. D.; Jensen, H. J. A.; Kongsted, J. *International Journal of Quantum Chemistry* **2014**, *114*, 1102–1107.
- (19) Stein, C. J.; Reiher, M. *Journal of Chemical Theory and Computation* **2016**, *12*, 1760–1771.
- (20) Su, J.; Xu, W.-H.; Xu, C.-F.; Schwarz, W. H. E.; Li, J. *Inorganic Chemistry* **2013**, *52*, 9867–9874.
- (21) Houmøller, J.; Kaufman, S. H.; Støchkel, K.; Tribedi, L. C.; Nielsen, S. B.; Weber, J. M. *ChemPhysChem* **2013**, *14*, 1133–1137.

- (22) Seth, M.; Ziegler, T.; Banerjee, A.; Autschbach, J.; van Gisbergen, S. J. A.; Baerends, E. J. J. *Chem. Phys.* **2004**, *120*, 10942–10954.
- (23) Savin, A. In *Recent Developments and Applications of Modern Density Functional Theory*; Elsevier: Amsterdam, 1996; p 327.
- (24) Savin, A.; Flad, H.-J. *International Journal of Quantum Chemistry* **1995**, *56*, 327–332.
- (25) Leininger, T.; Stoll, H.; Werner, H.-J.; Savin, A. *Chem. Phys. Lett.* **1997**, *275*, 151.
- (26) Ángyán, J. G.; Gerber, I. C.; Savin, A.; Toulouse, J. *Phys. Rev. A* **2005**, *72*, 012510.
- (27) Fromager, E.; Toulouse, J.; Jensen, H. J. A. *The Journal of Chemical Physics* **2007**, *126*, 074111.
- (28) Fromager, E.; Jensen, H. J. A. *Phys. Rev. A* **2008**, *78*, 022504.
- (29) Fromager, E.; Cimiraglia, R.; Jensen, H. J. A. *Phys. Rev. A* **2010**, *81*, 024502.
- (30) Toulouse, J.; Gerber, I. C.; Jansen, G.; Savin, A.; Ángyán, J. G. *Phys. Rev. Lett.* **2009**, *102*, 096404.
- (31) Fromager, E.; Knecht, S.; Jensen, H. J. A. *The Journal of Chemical Physics* **2013**, *138*, 084101.
- (32) Hedegård, E. D.; Heiden, F.; Knecht, S.; Fromager, E.; Jensen, H. J. A. *The Journal of Chemical Physics* **2013**, *139*, 184308.
- (33) Hedegård, E. D.; Knecht, S.; Kielberg, J. S.; Jensen, H. J. A.; Reiher, M. *The Journal of Chemical Physics* **2015**, *142*, 224108.
- (34) Hedegård, E. D. *Molecular Physics*.
- (35) Hubert, M.; Hedegård, E. D.; Jensen, H. J. A. *Journal of Chemical Theory and Computation* **2016**, *12*, 2203–2213, PMID: 27058733.

- (36) Hubert, M.; Jensen, H. J. A.; Hedegård, E. D. *The Journal of Physical Chemistry A* **2016**, *120*, 36–43, PMID: 26669578.
- (37) Senjean, B.; Hedegård, E. D.; Alam, M. M.; Knecht, S.; Fromager, E. *Molecular Physics* **2016**, *114*, 968–981.
- (38) Grimme, S.; Waletzke, M. *The Journal of Chemical Physics* **1999**, *111*, 5645–5655.
- (39) Marian, C. M.; Gilka, N. *Journal of Chemical Theory and Computation* **2008**, *4*, 1501–1515.
- (40) Manni, G. L.; Carlson, R. K.; Luo, S.; Ma, D.; Olsen, J.; Truhlar, D. G.; Gagliardi, L. *Journal of Chemical Theory and Computation* **2014**, *10*, 3669–3680.
- (41) Garza, A. J.; Bulik, I. W.; Henderson, T. M.; Scuseria, G. E. *Phys. Chem. Chem. Phys.* **2015**, *17*, 22412–22422.
- (42) Olsen, J. M.; Aidas, K.; Kongsted, J. *J. Chem. Theory Comput.* **2010**, *6*, 3721–3734.
- (43) Olsen, J. M.; Kongsted, J. *Adv. Quantum Chem.* **2011**, *61*, 107–143.
- (44) Hedegård, E. D.; Olsen, J. M. H.; Knecht, S.; Kongsted, J.; Jensen, H. J. A. *The Journal of Chemical Physics* **2015**, *142*, 114113.
- (45) Heyd, J.; Scuseria, G. E.; Ernzerhof, M. *The Journal of Chemical Physics* **2003**, *118*, 8207–8215.
- (46) Ballhausen, C. J. *Theoretica chimica acta* **1963**, *1*, 285–293.
- (47) Viste, A.; Gray, H. B. *Inorganic Chemistry* **1964**, *3*, 1113–1123.
- (48) Day, P.; Disipio, L.; Oleari, L. *Chemical Physics Letters* **1970**, *5*, 533 – 536.